

# A Generalized Magnetostrictive-Forces Approach to the Computation of the Magnetostriction-Induced Vibration of Laminated Steel Structures

Matija Javorski, Gregor Čepon, Janko Slavič, and Miha Boltežar

Faculty of Mechanical Engineering, University of Ljubljana, 1000 Ljubljana, Slovenia

November 2013

Cite as:

**Matija Javorski, Gregor Čepon, Janko Slavič, and Miha Boltežar**

**A Generalized Magnetostrictive-Forces Approach to the Computation of the Magnetostriction-Induced Vibration of Laminated Steel Structures**

**IEEE Transactions on Magnetics, Vol. 49, No. 11, November 2013.**

**DOI: [dx.doi.org/10.1109/TMAG.2013.2269316](https://doi.org/10.1109/TMAG.2013.2269316)**

This research introduces a new, numerical and experimental approach to the analysis of the vibration of laminated structures resulting from magnetostriction. The focus is on the in-plane magnetostriction of electrical steel and its transmission into the out-of-plane direction, in which laminated structures (e.g., transformer cores, stators, and rotors) exhibit the greatest vibration. A finite-element magnetostriction model is developed on an experimental basis and enables a general, in-plane and out-of-plane assessment of the magnetostrictive response. The magnetostriction model is compatible with various finite-element structural models and is incorporated into a structural model, updated based on experimental data, representing a clamped laminated structure. An experiment employing the operating-deflection-shapes method is used to assess the presented approach under various operating conditions.

*Index Terms*—Experiment, Finite-element methods, Laminated structure, Magnetostriction, Structural vibrations.

## I. INTRODUCTION

THE AC MAGNETOSTRICTION of electrical steel is a phenomenon accompanying the magnetisation process and often presents problems in terms of vibrations and the generation of noise. In the field of electrical machines, magnetostriction is recognized as one of the main causes of noise emissions [1], [2], [3], together with the Lorentz and reluctance magnetic forces. In the case of modern power transformers with multistep-lap cores, magnetostriction is reported to have the dominant effect [4]. This research introduces a new, numerical and experimental approach to the analysis of the vibration of electrical-steel structures resulting from magnetostriction.

In the field of numerical analysis, the finite-element method has proven suitable for modelling coupled magneto-mechanical problems because of its robustness and general applicability. A common approach to incorporating the effect of magnetostriction on the material is through a set of magnetostrictive forces (i.e., mechanical forces, which produce the same deformation of the material as does the magnetostriction [3], [5]). According to the review by Belahcen [6], the magnetostriction models are either force- or elongation-based.

Force-based models [3], [7] employ the principle of virtual work to determine the set of magnetostrictive forces from the magnetic field. This is similar to the way reluctance magnetic forces are calculated. However, as Belahcen pointed out [6] “the accuracy of this method relies on accurate measurements of the magnetization of iron sheets under an applied mechanical stress, not only unidirectional, but also multidirectional stress”. Due to the non-linear relations, this method has so far been limited to static [7] and transient dynamic analyses [3]. Harmonic analysis, which is important in the research on vibrations, has not yet been performed.

On the other hand, elongation-based models [8], [9], [10], [11] employ experimental data from magnetostrictive elongation to calculate the corresponding set of magnetostrictive forces through the stress-strain constitutive relations. In contrast to the force-based models, harmonic analyses are not uncommon in the case of the elongation-based models [8], [10], [11].

The relation between the ac magnetic flux density (sinusoidal waveform) and the ac magnetostriction is nonlinear, both in terms of amplitude and frequency [12]. In order to perform a harmonic mechanical analysis with magnetostriction as the excitation, this relation needs to be analytically approximated. In approaches to harmonic analysis, a quadratic approximation is

by far the most common [8], [10]. In this way the fundamental magnetostriction harmonic, featuring double the frequency of the magnetic field, is considered and other higher harmonics are not. To take the latter into account, Hilgert *et al.* [11] used two different models, i.e., a cubic-spline- and a neural-network-based approximation. The latter was found to be favourable since the neural network directly calculates the amplitudes and phases of the harmonics, thus taking account of the hysteresis effect as well.

The magnetostriction-induced vibration of an electrical-steel component (e.g., a transformer core, a stator or a rotor of an electric motor) is distinct for the following reason: whereas the excitation occurs in the plane of the sheets, the laminated structure is most flexible in the sheet's normal direction and an out-of-plane vibration often dominates [13], [14]. Models addressing this cross-axis coupling are rare and not suitable for general application. Kubiak and Witczak [13] took the macroscopic asymmetry of the transformer core to produce the out-of-plane excitation. Li *et al.* [15] employed an energy-conservation principle to determine the equivalent magnetostrictive force, generating the out-of-plane vibration of an electrical-steel plate. However, the natural dynamics of the plate was not included, thus limiting the applicability of the approach.

The generalized magnetostrictive-forces approach introduced in this paper provides a universal method for the in-plane and out-of-plane magnetostriction-induced vibration analysis. The approach is elongation-based, regarding the experimental relations between the magnetic flux density and the magnetostrictive strain, to calculate the mechanical excitation. Analytical approximations are made for the individual harmonics of magnetostriction, translating the problem into the framework of a linear harmonic analysis. On the basis of the in-plane magnetostriction, the out-of-plane excitation mechanism is derived, taking into account the heterogeneous grain structure of the material. The complex coupling between the in- and the out-of-plane directions is identified experimentally. The magnetostriction model is element-based and can be implemented on various structural finite-element models of electrical-steel structures. In this research, analysing a clamped laminated structure, the method by Pirnat *et al.* [16] was adopted to create an updated structural model. An experiment employing the operating-deflection-shapes method [17] is used to assess the numerical approach under a variable magnetic excitation, materials with various magnetostrictive characteristics and the structures of different natural dynamics.

This manuscript is organized as follows. The theoretical background to the method of analysis is given in Section II. Section III presents the application of the method on a purpose-built experimental set-up. The conclusions are drawn in the final section.

## II. METHOD OF ANALYSIS

The numerical analysis of the magnetostriction-induced vibration is based on the finite-element method. This section presents the structural and magnetostriction models employed in this study.

### A. Structural Model

The mechanical properties of structures made of electrical steel are greatly influenced by the material itself and the technique used to assemble them. Since power-transformer cores and electric-motor stators and rotors are manufactured as stacks of electrical steel laminations, the interlaminar contact, in particular, has a significant effect. This research deals with the case of laminated stacks that are clamped together to provide dry friction between the laminations.

The method presented by Pirnat *et al.* [16] was adopted to provide an updated structural model of the laminated structure. The laminations are modelled individually using shell elements and the orthotropic behaviour of the material is taken into account. As described in [16], the contact problem is solved using a two-stage formulation. In stage I the nodes of the adjacent laminations are connected using nonlinear link elements, representing the nonlinear stiffness of the stack in the normal direction. On the basis of the clamping forces, the distribution of the interlaminar pressure  $p$  is computed. In stage II, the link elements are replaced with linear beam elements, modelling the linearized stiffness in the normal direction  $k_N$  as well as the contact stiffness  $k$  and the damping  $d$  in the in-plane direction (Fig. 1). A linear friction contact law is implemented, assuming  $k$  and  $d$  are proportional to the surface pressure  $p$ . The ratios  $k/p$  and  $d/p$  are determined on the basis of the experimental data for the structure's natural dynamics.

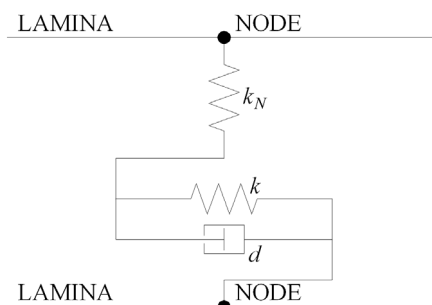


Fig. 1. Model of the interlaminar contact.

### B. Magnetostriction Model

The generalized magnetostrictive-forces approach operates at the level of a single finite element. The mechanical excitation for the element in question is determined on the basis of the magnetic field and the experimentally identified magnetostrictive characteristics.

#### 1) In-plane Vibration

The in-plane magnetostrictive forces are used to represent the effect of the magnetostriction on the in-plane vibration of the selected finite element. The forces are calculated in the following way. Firstly, the deformation of a free (no boundary conditions) finite element is established, based on the magnetic flux density and the experimental magnetostriction data. Secondly, the mechanical forces needed to deform the element back into its original shape are calculated. Finally, the magnetostrictive forces are found as the reactions to these mechanical forces. This principle is analogous to the way that thermal strains are modelled. It should be pointed out that whereas the magnetostrictive forces produce the correct in-plane strain field, this is not true for the stress field and an erroneous result is possible in specific cases (e.g., in buckling under in-plane compression).

For a mechanically orthotropic material, like electrical steel, the in-plane, stress-strain constitutive relations may be written in matrix form [18]:

$$\begin{bmatrix} \sigma_x \\ \sigma_y \\ \tau_{xy} \end{bmatrix} = \frac{1}{1 - \nu_{xy}\nu_{yx}} \begin{bmatrix} E_x & \nu_{xy}E_y & 0 \\ \nu_{yx}E_x & E_y & 0 \\ 0 & 0 & (1 - \nu_{xy}\nu_{yx})G_{xy} \end{bmatrix} \begin{bmatrix} \varepsilon_x \\ \varepsilon_y \\ \gamma_{xy} \end{bmatrix}, \quad (1)$$

where  $\sigma$  is the normal stress,  $\tau$  is the shear stress,  $\nu$  is the Poisson's ratio,  $E$  is the elastic modulus,  $G$  is the shear modulus,  $\varepsilon$  is the normal strain and  $\gamma$  is the shear strain.  $x$  denotes the in-plane rolling direction of the steel sheet and  $y$  the in-plane transverse direction. This research focuses on the case of the magnetic flux density vector occurring parallel to the rolling direction. Therefore, the magnetostriction can be assumed to produce no shear strain  $\gamma_{xy} = \tau_{xy} = 0$  [19]. The magnetostrictive strain in the direction that is normal to the steel plane (out-of-plane direction  $z$ ) is not considered in this research.

The magnetostriction model takes account of each harmonic of the magnetostriction separately. Based on the experimental data of single-axis measurements (experimental method presented by Javorski *et al.* [20]), the following power approximation was found to accurately characterize the amplitudes of the harmonics:

$$\varepsilon_x = k_{\varepsilon_x} B_x^{n_x}, \quad n_x = 2i, \quad (2)$$

where  $B_x$  is the amplitude of the magnetic flux density,  $k_{\varepsilon_x}$  is the magnetostriction coefficient and  $n_x$  is the power of the approximation for the rolling direction.  $i$  is a natural number. Whereas the power  $n_x$  defines the particular function type, used for the approximation (e.g., quadratic, quartic...), the coefficient  $k_{\varepsilon_x}$  specifies the proportionality between the function type and the experimental data. The values of  $k_{\varepsilon_x}$  and  $n_x$  are selected for the approximation that best fits the experimental data.

If we assume that magnetostriction is an isochoric process [21], the ratio between the strain in the direction perpendicular to the magnetisation and the strain in the magnetisation direction is known:

$$\nu_{MS} = 1/2. \quad (3)$$

This allows the amplitude of the magnetostrictive strain in the in-plane transverse direction to be written:

$$\varepsilon_y = -\nu_{MS}\varepsilon_x = -\nu_{MS}k_{\varepsilon_x} B_x^{n_x}, \quad n_x = 2i. \quad (4)$$

At the level of a single finite element the magnetic solution of  $B_x$  is used together with the experimentally identified parameters  $k_{\varepsilon_x}$  and  $n_x$  to calculate the components of strain  $\varepsilon_x$  and  $\varepsilon_y$  - (2) and (4). The latter are used in (1) to derive the corresponding mechanical stresses  $\sigma_x$  and  $\sigma_y$ . Finally, these stresses are transformed into nodal forces ( $F_x$  and  $F_y$ ) according to the principles of the finite-element method. The magnetostrictive in-plane nodal forces on a single finite element are presented in Fig. 2.

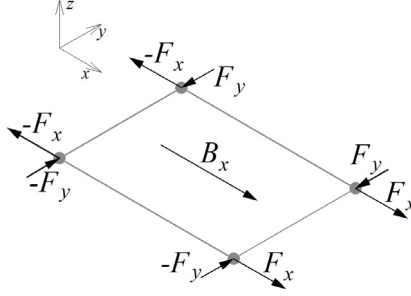


Fig. 2. Magnetostrictive in-plane nodal forces on a single finite element.

## 2) Out-of-plane Vibration

As was pointed out in the Introduction, in-plane magnetostriction often results in a pronounced out-of-plane vibration [13], [14]. The research by Weiser *et al.* [4] focused on the mechanisms of noise generation in transformer cores, and showed dominant out-of-plane vibration in the case of a tightly compressed, multistep-lap core. According to the authors, magnetostriction is the single most important excitation mechanism of such a structure. Dynamical coupling between the in-plane and the out-of-plane directions was also demonstrated in the research by Javorski *et al.* [20], which focused on the dynamic suitability of magnetostriction-measurement set-ups. It is clear that out-of-plane vibration is intrinsic to in-plane magnetostriction.

The heterogeneous grain structure of an electrical steel is assumed to be the source of the coupling between the in-plane and out-of-plane directions. Namely, under magnetization the individual grains exhibit different magnetostrictive deformations; this being predominantly due to the different crystal orientations [22]. As a result of the incompatibilities between the grains, magnetostrictive strain is always accompanied by an additional elastic strain. In this research we assumed that this elastic strain manifests itself not only in the in-plane direction, but also in the out-of-plane direction. In short, along with the in-plane grain magnetostriction of  $\Delta l$ , an additional out-of-plane deformation of  $\Delta w$  occurs. This out-of-plane deformation is assumed proportional to the magnetostriction  $\Delta l$ . The deformation of a single grain of electrical steel is presented in Fig. 3, where  $B$  is the magnetic flux density and  $l$  is the length of the grain.

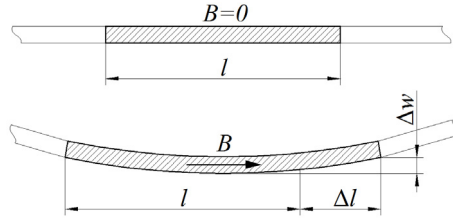


Fig. 3. Magnetostrictive deformation of a single grain of electrical steel.

Whereas the in-plane model considers the macroscopic characteristics of magnetostriction (averaged over the grain structure), the out-of-plane model is founded on the presented local effect. For this reason, the finite-element mesh is set to correspond to the grain structure of the material with the element dimensions being of the same order as the average grain dimensions. Finite elements representing individual grains are not uncommon in magnetostriction models, although they are used for different purposes (e.g., averaging the magnetostrictive behaviour of the grains [22], [23]). In the approach introduced here, such an element mesh is subjected to out-of-plane nodal forces and in-plane nodal moments to generate the out-of-plane deformation - Fig. 4. Because the deformation is assumed to occur on the scale of the grains, the nodal forces and moments are set to alternate between the elements in a chess-pattern manner. In this way a static equilibrium is also maintained. The amplitude of the out-of-plane nodal forces is estimated with:

$$F_z = k_F \sqrt{F_x^2 + F_y^2}, \quad (5)$$

where  $k_F$  is the force-proportionality factor.

The amplitude of the in-plane nodal moments is estimated with:

$$M_x = M_y = k_M \sqrt{F_x^2 + F_y^2}, \quad (6)$$

where  $k_M$  is the moment-proportionality factor. Using (5) and (6) a generalized linear relation is established between the in-plane and the out-of-plane deformations. Due to the complexity of the coupling between the two directions, the proportionality factors  $k_F$  and  $k_M$  are identified experimentally.

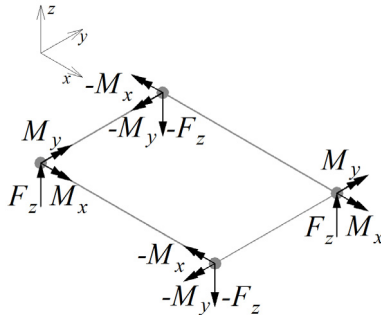


Fig. 4. Magnetostrictive out-of-plane nodal forces and in-plane nodal moments on a single finite element.

It should be pointed out that the introduced concept of out-of-plane deformation does not originate from experimental identification of the magnetostriction of individual grains. It was assumed on the basis of global magnetostrictive response of electrical-steel structures to enable modelling the transmission of the in-plane magnetostriction into the out-of-plane direction.

### III. APPLICATION OF THE METHOD

An experiment involving magnetostriction-induced vibration was conducted to provide reference data for the presented numerical method. A sinusoidal magnetic field with a frequency of 50 Hz and various flux densities was used to generate magnetostriction in the electrical steel. In accordance with the magnetostriction model, the magnetic field was oriented in the in-plane rolling direction of the material ( $x$ ). The research was focused on the magnetostriction harmonics of 100 and 200 Hz as their considerable amplitudes proved advantageous to the quality of the measurement.

#### A. Test Object

Two stacks of electrical steel sheets were used as the test objects. The stacks were made of 15 sheets of grain-oriented electrical steel, each sheet measuring 180 mm x 40 mm x 0.27 mm. Different grades of material were used for the stacks to provide dissimilar magnetostrictive behaviours. The sheets were compressed together using clamps with bolt fastenings. The clamping torque was controlled using a precision torque wrench. The relation between the torque and the corresponding clamping force was determined with a separate experiment. Different numbers of clamps and different clamping forces were used to create dissimilar natural dynamics for the two stacks. The used lamina surface pressure was in the range of typical values for the majority of electrical-steel components. Details of the stacks are presented in Table I.

TABLE I  
THE ANALYSED STACKS

	Grade – standard EN 10107:2005	Number of clamps	Clamping torque	Clamping force
Stack A	M 103-27 P	5	1.2 N·m	398 N
Stack B	M 90-27 P	3	0.4 N·m	236 N

#### B. Experimental Analysis of the Magnetostriction-Induced Vibration

An experimental set-up (Fig. 5) was used to provide controlled magnetostrictive excitation of the test stacks and to determine the stack's response. In the set-up, the stack was suspended using a couple of strings, emulating free-free boundary conditions. To form a closed path for the magnetic flux, a ferromagnetic yoke was used, with ferrous powder sacks positioned at the interface between the test stack and the yoke. The sacks were used to bridge any air gaps that might otherwise arise as a result of the vibration of the stack. Also, the sacks have a minimal mechanical influence on the stack, as will be evident from the results.

A PC running a custom-designed measurement application was used to perform the measurement. The magnetisation signal was generated with a 16-bit analogue signal generator, amplified with a 1-kW laboratory power amplifier and applied to the magnetising coil (550 turns), positioned on the yoke. The magnetic flux density in the stack was monitored with a search coil (1 turn) that was tightly wound around the sample to minimize the influence of the air flux. A 16-bit analogue input module, running at a 5-kHz sampling frequency, was used to acquire the signal from the search coil. The reading was used in a feedback loop for the control of the magnetisation signal.

The mechanical response of the stack was measured using the operating deflection-shapes method [17]. Effectively, this

method sorts the resulting movement of the structure into individual frequency components. A laser Doppler velocimeter (sensitivity 0.2 V/(mm/s)) was used to measure the out-of-plane response of the stack. The measurement was performed at 26 measurement points, arranged in a grid of 2x13 points. The velocity signal was acquired using a 24-bit analogue input module, running at a 5-kHz sampling frequency.

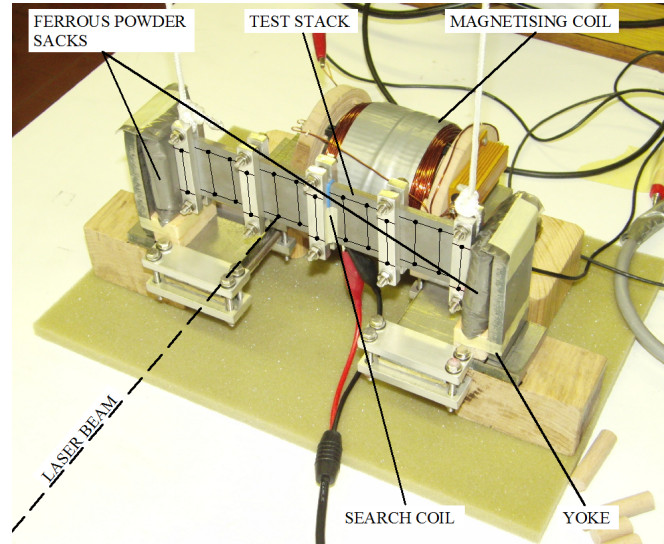


Fig. 5. Set-up for the measurement of the operating deflection shapes.

### C. Numerical Analysis of the Magnetostriction-Induced Vibration

The operation of the experimental set-up was analysed numerically using the two-stage approach to structural modelling (Section II.A) and the introduced, generalized magnetostrictive-forces approach (Section II.B). Steps of the procedure for the numerical analysis are schematically presented in Fig. 6.

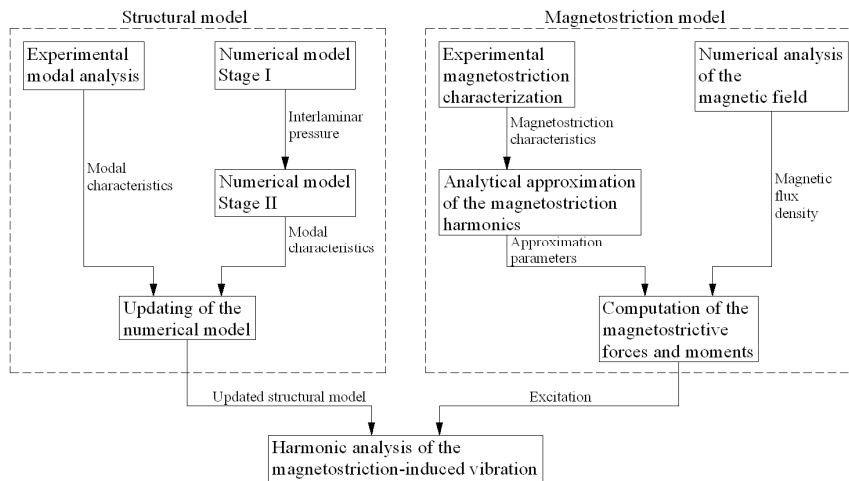


Fig. 6. Steps of the procedure for the numerical analysis.

#### 1) Structural Model

The structural model is required to reflect the essential modal characteristics of the analysed structure (the test stack), i.e., the eigenmodes with corresponding natural frequencies and damping ratios. Therefore, these characteristics were identified using an experimental modal analysis [24]. The same grid of 26 measurement points as in operating-deflection-shapes analysis was used. The system was excited with an electrodynamic shaker and the excitation force was monitored with a force transducer (sensitivity 1.2 mV/N). A roving piezoelectric accelerometer (sensitivity 10 mV/(m/s<sup>2</sup>)) was used to measure the response at the measurement points. The signals of the two sensors were acquired using a 24-bit analogue input module, running at a 25.6-kHz sampling frequency. A PC running a custom-designed measurement application was used to perform the measurement and to compute the required modal parameters. The set-up for the experimental modal analysis is presented in Fig. 7.

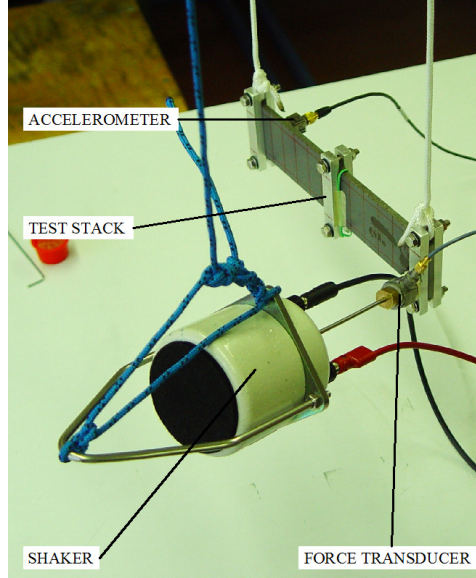


Fig. 7. Set-up for the experimental modal analysis.

The experimentally identified modal characteristics enabled an updated numerical model of the structure to be created. Modelling was performed using the ANSYS finite-element analysis package. The individual laminations were modelled using 8-node structural SHELL281 elements since this element type is intended for mechanical analyses of thin to moderately thick shell structures. The element size was set to 5 mm x 5 mm x 0.27 mm, which corresponds to the mm-sized grains reported for the grain-oriented electrical steel [22]. Twenty-node structural SOLID95 elements were used for the clamps and nonlinear LINK8 elements were used to represent the interlaminar contact in stage I of the numerical model. The stiffness of the links was determined on the basis of the experimentally assessed compression characteristic of the stack. Under known clamping forces, a nonlinear static analysis was performed to establish the interlaminar pressure distribution. This was followed by stage II of structural modelling, where BEAM4 elements were used instead of the links. Following the method from Section II.A, the in-plane contact stiffness  $k$  and the damping  $d$  were set to be proportional to the contact pressure  $p$  with the ratios  $k/p$  and  $d/p$  calibrated with respect to the experiment. Also, in the second stage, the nonlinear compression characteristic of the stack was linearized. This allowed a linear modal analysis of the structure to be made. The first two bending modes of the structure were considered when updating the numerical model. A comparison with the experiment is presented in Tables II and III. Relative error between experimental ( $f_{EXP}$ ) and numerical natural frequency ( $f_{NUM}$ ) is determined as:

$$\eta_f = \frac{|f_{EXP} - f_{NUM}|}{f_{EXP}} \cdot 100\% \quad (7)$$

and the relative error between experimental ( $\xi_{EXP}$ ) and numerical damping ratio ( $\xi_{NUM}$ ) is determined as:

$$\eta_\xi = \frac{|\xi_{EXP} - \xi_{NUM}|}{\xi_{EXP}} \cdot 100\%. \quad (8)$$

Relatively good agreement was achieved in terms of the natural frequencies, with the average relative error of 6%, while an acceptable agreement was achieved in terms of the damping ratios, with the average relative error of 34%.

TABLE II  
COMPARISON OF THE NATURAL FREQUENCIES

	Bending mode	$f_{EXP}$ [Hz]	$f_{NUM}$ [Hz]	$\eta_f$ [%]
Stack A	1	112.2	110.3	1.7
	2	169.8	173.6	2.2
Stack B	1	54.5	64.1	17.6
	2	213.5	204.7	4.1

$f_{EXP}$  - experimental natural frequency [Hz]

$f_{NUM}$  - numerical natural frequency [Hz]

$\eta_f$  - frequency relative error [%]

TABLE III  
COMPARISON OF THE DAMPING RATIOS

	Bending mode	$\xi_{EXP}$ [%]	$\xi_{NUM}$ [%]	$\eta_\xi$ [%]
Stack A	1	5.1	5.1	0.2
	2	5.3	5.4	1.1
Stack B	1	2.1	0.6	72.0
	2	4.6	7.5	62.1

$\xi_{EXP}$  - experimental damping ratio [%]

$\xi_{NUM}$  - numerical damping ratio [%]

$\eta_\xi$  - damping-ratio relative error [%]

## 2) Magnetostriction Model

The input parameters for the magnetostriction model are the in-plane magnetostriction characteristics and the magnetic field solution. The in-plane magnetostriction was characterized using the single-axis measurement system presented in [20]. The relation between the amplitude of the magnetic flux density and the magnetostriction harmonics was approximated in accordance with (2). The method of least squares was used to select the best fitting approximation - Fig. 8. depicts the comparison of the experimental data and the approximation for stack B. The identified magnetostriction parameters are presented in Table IV. The proportionality factors  $k_F$  and  $k_M$  for the out-of-plane excitation were set with regards to the results of the operating-deflection-shapes analysis.

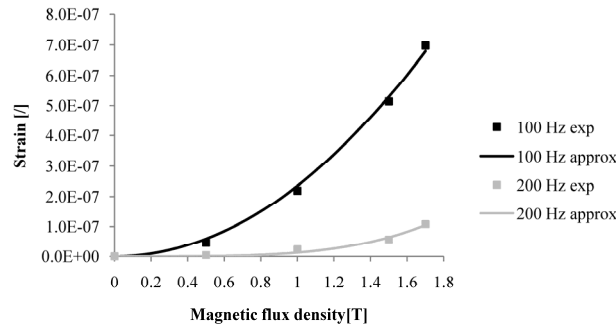


Fig. 8. Approximation of the 100- and 200-Hz harmonics for stack B.

TABLE IV  
MAGNETOSTRICTION APPROXIMATION PARAMETERS

	Harmonic	$k_{\epsilon_x}$ [ $T^{-n_x}$ ]	$n_x$ [I]
Stack A	100 Hz	$4.96 \times 10^{-7}$	2
	200 Hz	$6.89 \times 10^{-8}$	2
Stack B	100 Hz	$2.35 \times 10^{-7}$	2
	200 Hz	$1.26 \times 10^{-8}$	4

$k_{\epsilon_x}$  - magnetostriction coefficient [ $T^{-n_x}$ ]

$n_x$  - power of the approximation [I]

The next step in the procedure was the assessment of the magnetic field. The experimental set-up was modelled in 3D using a twenty-node electromagnetic SOLID236 element with either a brick or tetrahedral shape. In accordance with the element-based approach, the same mesh of the stack as in the structural model was used for the magnetic analysis. The used element type

proved suited to modelling the laminations, taking into account the magnetisation curve as well as the magnetic orthotropy of the material. A time-stepping transient analysis was performed with the results for  $B_x$  acquired for each of the elements of the test stack.

#### D. Assessment of the Numerical Method

Joint use of the structural model and the magnetostriction model made it possible to perform numerical analyses of the magnetostriction-induced vibration of the two stacks. Firstly, to demonstrate the method accounts for variable magnetic excitation, stack A was analysed under three amplitudes of magnetic flux density, i.e., 1.0, 1.5 and 1.7 T. Secondly, to demonstrate the method also accounts for materials of various levels of magnetostriction performance and structures of different natural dynamics, stack B was analysed under 1.5 T. The harmonic excitations of 100 and 200 Hz were considered individually in a linear harmonic analysis. The mechanical response due to the reluctance magnetic forces was numerically estimated to be less than 1% of the total response, and on this basis it was neglected. The proportionality factors  $k_F$  and  $k_M$ , characterizing the coupling between the in- and out-of-plane vibrations, were calibrated with respect to the experimentally identified response. The factors were determined for  $k_F = 0.04$  and  $k_M = 0.002$  m.

The amplitude of the out-of-plane response was measured as the mean distance between the antinodes of opposite deflection. The results for the deformation amplitude are presented in Table V. Relative error between experimental ( $Z_{EXP}$ ) and numerical deformation amplitude ( $Z_{NUM}$ ) is determined as:

$$\eta_Z = \frac{|Z_{EXP} - Z_{NUM}|}{Z_{EXP}} \cdot 100\%. \quad (9)$$

The average relative error between experimental and numerical deformation amplitude is 30%.

The vibration modes of the stacks are presented in Figs. 9-12. The shape of the modes is compared using the modal assurance criterion (MAC) [24].

TABLE V  
DEFORMATION AMPLITUDE

	$B_x$ [T]	$f$ [Hz]	$Z_{EXP}$ [m]	$Z_{NUM}$ [m]	$\eta_Z$ [%]
Stack A	1.0	100	$0.62 \times 10^{-5}$	$1.06 \times 10^{-5}$	71.0
	1.0	200	$3.11 \times 10^{-7}$	$3.43 \times 10^{-7}$	10.3
Stack A	1.5	100	$1.87 \times 10^{-5}$	$2.36 \times 10^{-5}$	26.2
	1.5	200	$11.0 \times 10^{-7}$	$7.38 \times 10^{-7}$	32.9
Stack A	1.7	100	$2.41 \times 10^{-5}$	$2.87 \times 10^{-5}$	19.1
	1.7	200	$7.54 \times 10^{-7}$	$9.62 \times 10^{-7}$	27.6
Stack B	1.5	100	$0.77 \times 10^{-5}$	$0.53 \times 10^{-5}$	31.2
	1.5	200	$6.42 \times 10^{-7}$	$5.23 \times 10^{-7}$	18.5

$B_x$  - magnetic flux density amplitude [T]

$f$  - frequency [Hz]

$Z_{EXP}$  - experimental deformation amplitude [m]

$Z_{NUM}$  - numerical deformation amplitude [m]

$\eta_Z$  - amplitude relative error [%]

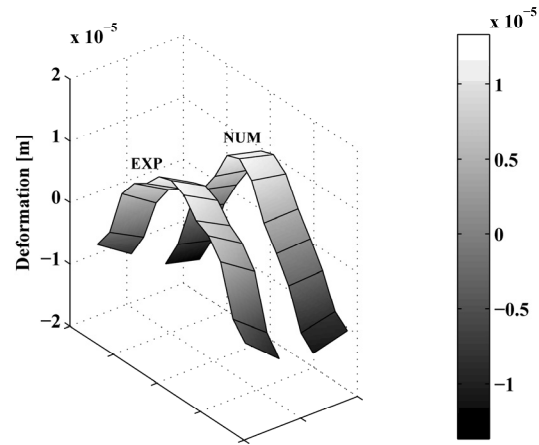


Fig. 9. Stack A: 100-Hz component of the out-of-plane response at 1.5 T. Experiment – left, numerical solution – right. MAC = 0.71.

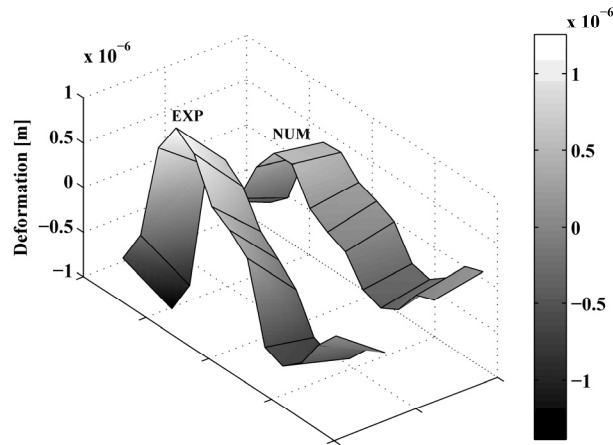


Fig. 10. Stack A: 200-Hz component of the out-of-plane response at 1.5 T. Experiment – left, numerical solution – right. MAC = 0.55.

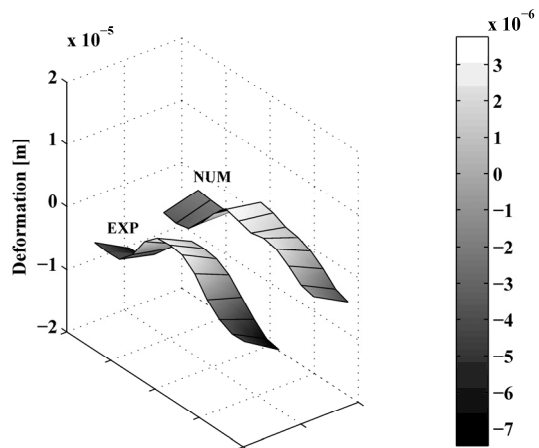


Fig. 11. Stack B: 100-Hz component of the out-of-plane response at 1.5 T. Experiment – left, numerical solution – right. MAC = 0.54.

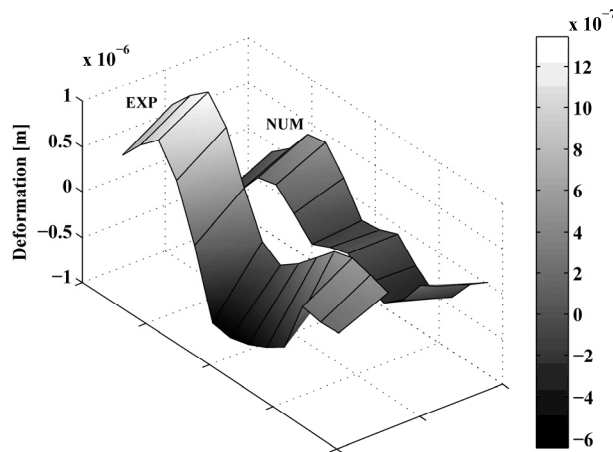


Fig. 12. Stack B: 200-Hz component of the out-of-plane response at 1.5 T. Experiment – left, numerical solution – right. MAC = 0.25.

#### IV. CONCLUSIONS

A new, generalized magnetostrictive-forces approach is introduced for a numerical analysis of the magnetostriction-induced vibration in electrical-steel structures. This approach takes into account the frequency composition of the magnetostriction by introducing generally applicable analytical approximations for the harmonics.

The developed magnetostriction model is element-based and compatible with various structural models for a finite-element analysis. A structural model, accounting for the interlaminar contact and the mechanical orthotropy, was set up according to [16] and updated, based on experimental modal analysis.

For the magnetostriction model, a mechanism of out-of-plane excitation was devised together with the in-plane excitation. Material heterogeneity was assumed to transmit some of the in-plane magnetostriction into the out-of-plane direction. Due to the complexity of the problem, an empirical approach was adopted, using the experimentally identified factors  $k_F$  and  $k_M$  as measures of this cross-axis coupling. The values of 0.04 and 0.002 m seem reasonable, since in this way only a fraction of the in-plane excitation is transmitted. However, due to the pronounced out-of-plane flexibility and the natural dynamics of the test structure, the out-of-plane response was up to two orders greater than the in-plane vibration. This additionally indicates the importance of research on the cross-axis transmission of vibrations.

When comparing the experimental and the numerical response, relatively poor agreement can be attributed to the stack B at 1.5 T and 200 Hz (Fig. 12). This is due to the presence of rigid body motion, presenting a disturbance to the experiment and particularly affecting the MAC criterion.

Despite some discrepancies, a correlation in both the deformation amplitude and the shape is evident throughout the range of the disclosed results. In this way, the generalized magnetostrictive-forces approach presents a certain level of general applicability, since variable magnetic excitation as well as materials with various levels of magnetostriction performance and stacks of different natural dynamics were assessed. Presenting a limiting factor to the approach is the need for experimental identification of the proportionality factors  $k_F$  and  $k_M$ , when analysing a new type of structure.

Considering the development of the approach, further work is also required on the identification of the relations between the structure parameters (lamination thickness, stack dimensions, grain size) and the finite-element mesh characteristics (element shape and size).

#### REFERENCES

- [1] P. I. Anderson, A. J. Moses, and H. J. Stanbury, "Assessment of the stress sensitivity of magnetostriction in grain-oriented silicon steel," *IEEE Trans. Magn.*, vol. 43, no. 8, pp. 3467-3476, Aug. 2007.
- [2] C. G. Kim, H. C. Kim, S. J. Ahn, S. Y. Cha, and S. K. Chang, "Magnetizing angle dependence of harmonics of magnetic induction and magnetostriction in electrical steel," *J. Magn. Magn. Mater.*, vol. 215-216, pp. 159-161, June 2000.
- [3] O. A. Mohammed, T. E. Calvert, L. Petersen, and R. McConnell, "Transient Modeling of Coupled Magnetoelastic Problems in Electric Machines," in *Power Engineering Society Summer Meeting, 2002 IEEE*, Chicago, IL, 2002, vol.1, pp. 281-287.
- [4] B. Weiser, H. Pfützner, and J. Anger, "Relevance of Magnetostriction and Forces for the Generation of Audible Noise of Transformer Cores," *IEEE Trans. Magn.*, vol. 36, no. 5, pp. 3759-3777, Sept. 2000.
- [5] K. Delaere, W. Heylen, K. Hameyer, and R. Belmans, "Local magnetostriction forces for finite element analysis," *IEEE Trans. Magn.*, vol. 36, no. 5, pp. 3115-3118, Sept. 2000.
- [6] A. Belahcen, *Magnetoelasticity, magnetic forces and magnetostriction in electrical machines*, Ph.D. dissertation, Helsinki Univ. Tech., Espoo, Finland, 2004, unpublished.
- [7] M. Besbes, Z. Ren, and A. Razek, "Finite Element Analysis of Magneto-Mechanical Coupled Phenomena in Magnetostrictive Materials," *IEEE Trans. Magn.*, vol. 32, no. 3, pp. 1058-1061, May 1996.

- [8] S. D. Garvey and C. N. Glew, "Magnetostrictive excitation of vibration in machines – a modal approach," in *Ninth international Conference on Electrical Machines and Drives*, Canterbury, Kent, UK, 1999, Conf. Publ. No. 468, pp. 169-173.
- [9] L. Gros, G. Reyne, C. Body, and G. Meunier, "Strong Coupling Magneto Mechanical Methods Applied to Model Heavy Magnetostrictive Actuators," *IEEE Trans. Magn.*, vol. 34, no. 5, pp. 3150-3153, Sept. 1998.
- [10] W. Kitagawa, Y. Ishihara, T. Todaka, and A. Nakasaka, "Analysis of Structural Deformation and Vibration of a Transformer Core by Using Magnetic Property of Magnetostriction," *ELECTR ENG JPN*, vol. 172, no. 1, pp. 19-26, July 2010.
- [11] T. Hilgert, L. Vandavelde, and J. Melkebeek, "Comparison of Magnetostriction Models for Use in Calculations of Vibrations in Magnetic Cores," *IEEE Trans. Magn.*, vol. 44, no. 6, pp. 874-877, June 2008.
- [12] M. Hirano, Y. Ishihara, K. Harada, and T. Todaka, "A study on measurement of magnetostriction of silicon steel sheet by laser displacement meter," *J. Magn. Magn. Mater.*, vol. 254-255, pp. 43-46, Jan. 2003.
- [13] W. Kubiak and P. Witczak, "Vibration analysis of small power transformer," *COMPEL*, vol. 29, no. 4, pp. 1116-1124, 2010.
- [14] X. G. Yao, T. P. P. Phway, A. J. Moses, and F. Anayi, "Magneto-Mechanical Resonance in a Model 3-Phase 3-Limb Transformer Core Under Sinusoidal and PWM Voltage Excitation," *IEEE Trans. Magn.*, vol. 44, no. 11, pp. 4111-4114, Nov. 2008.
- [15] Q. Li, X. Wang, L. Zhang, J. Lou, and L. Zou, "Modelling methodology for transformer core vibrations based on the magnetostrictive properties," *IET Electr. Power Appl.*, vol. 6, no. 9, pp. 604-610, Nov. 2012.
- [16] M. Pirnat, G. Čepon, and M. Boltežar, "Introduction of the linear contact model in the dynamic model of laminated structure dynamics: an experimental and numerical identification," *Mech. mach. theory*, vol. 64, pp. 144-154, June 2013.
- [17] B. J. Schwarz and M. H. Richardson, "Introduction to operating deflection shapes," in *CSI Reliability Week*, Orlando, FL, 1999.
- [18] A. W. Leissa, "Appendix - Plate Equations," in *Vibration of Plates*. Washington, D.C.: NASA, 1969, pp. 335-336.
- [19] A. Belahcen, "Vibrations of Rotating Electrical Machines Due to Magnetomechanical Coupling and Magnetostriction," *IEEE Trans. Magn.*, vol. 42, no. 4, pp. 971-974, Apr. 2006.
- [20] M. Javorski, J. Slavič, and M. Boltežar, "Frequency Characteristics of Magnetostriction in Electrical Steel Related to the Structural Vibrations," *IEEE Trans. Magn.*, vol. 48, no. 12, pp. 4727-4734, Dec. 2012.
- [21] D. Jiles, "Magnetic Properties," in *Introduction to Magnetism and Magnetic Materials*. London, UK: Chapman and Hall, 1991, pp. 104.
- [22] R. Decoquer, L. Kestens, and Y. Houbaert, "Modelling the magnetostriction coefficient of polycrystalline ferromagnetic materials with a cubic structure by means of the finite element method," *J. Magn. Magn. Mater.*, vol. 242-245, pp. 1218-1220, Apr. 2002.
- [23] N. Buiron, L. Hirsinger, and R. Billardon, "A micro-macro model for magnetostriction and stress effect on magnetisation," *J. Magn. Magn. Mater.*, vol. 196-197, pp. 868-870, May 1999.
- [24] N. M. M. Maia et al., *Theoretical and Experimental Modal Analysis*. Baldock, Hertfordshire, UK: Research Studies Press Ltd., 1998.